

Cytolysin-dependent delay of vacuole maturation in macrophages infected with *Listeria monocytogenes*

Rebecca Henry,^{1,2} Lee Shaughnessy,¹
Martin J. Loessner,³ Christine Alberti-Segui,⁴
Darren E. Higgins⁴ and Joel A. Swanson^{1,2}

¹Department of Microbiology and Immunology and

²Program in Immunology, University of Michigan Medical School, Ann Arbor, MI 48109-0620, USA.

³Institute of Food Science and Nutrition, Swiss Federal Institute of Technology, CH-8092 Zurich, Switzerland.

⁴Department of Microbiology and Molecular Genetics, Harvard Medical School, Boston, MA 02115-6092, USA.

Summary

The bacterial pathogen *Listeria monocytogenes* (*Lm*) evades the antimicrobial mechanisms of macrophages by escaping from vacuoles to the cytosol, through the action of the cytolysin listeriolysin O (LLO). Because of heterogeneities in the timing and efficiency of escape, important questions about the contributions of LLO to *Lm* vacuole identity and trafficking have been inaccessible. Expression of cyan fluorescent protein (CFP)-labelled endocytic membrane markers in macrophages along with a yellow fluorescent protein (YFP)-labelled indicator of *Lm* entry to the cytosol identified compartments lysed by bacteria. *Lm* escaped from Rab5a-negative, lysosome-associated membrane protein-1 (LAMP1)-negative, Rab7-positive, phosphatidylinositol 3-phosphate [PI(3)P]-positive vacuoles. *Lm* vacuoles did not label with YFP-Rab5a unless the bacteria were first opsonized with IgG. Wild-type *Lm* delayed vacuole fusion with LAMP1-positive lysosomes, relative to LLO-deficient *Lm*. Bacteria prevented from expressing LLO until their arrival into LAMP1-positive lysosomes escaped inefficiently. Thus, the LLO-dependent delay of *Lm* vacuole fusion with lysosomes affords *Lm* a competitive edge against macrophage defences by providing bacteria more time in organelles they can penetrate.

Introduction

Macrophages play a vital role in the innate immune response by internalizing and destroying pathogenic

microbes by phagocytosis. Sequential interactions of the phagosome with the endocytic pathway lead to changes in the lipid and protein composition of its membrane (Desjardins *et al.*, 1994) and generation of molecules important for host defence, including reactive oxygen and nitrogen intermediates (Shiloh *et al.*, 1999). Eventually the phagosome fuses with lysosomes, intracellular compartments that contain hydrolases which destroy the phagosomal contents.

To successfully invade and replicate within macrophages, some intracellular pathogens employ mechanisms to avoid destruction in the harsh environment of lysosomes. The facultative intracellular pathogen *Listeria monocytogenes* (*Lm*) survives within macrophages by producing a cholesterol-dependent, pore-forming cytolysin, listeriolysin O (LLO), which perforates *Lm*-containing phagosomes (*Lm* vacuoles) and allows the bacteria to escape into the nutrient-rich macrophage cytosol (Portnoy *et al.*, 1988; Tweten *et al.*, 2001). After a period of growth in the cytosol, the bacteria recruit and polymerize host cell actin. Rocket-shaped tails of filamentous actin (F-actin) propel the bacteria into neighbouring cells, where the infectious cycle begins again (Cossart and Lecuit, 1998). Actin nucleation by cytosolic *Lm* is commonly used as an indicator of *Lm* escape (Jones and Portnoy, 1994).

Listeriolysin O is essential for *Lm* virulence. *Lm* lacking LLO (*hly* *Lm*) fail to escape vacuoles within macrophages and are avirulent (Portnoy *et al.*, 1988). LLO acts on the *Lm* vacuole soon after infection. Initial pore formation by LLO occurs within 5 min after internalization of the bacteria (Beauregard *et al.*, 1997), and escape of *Lm* to the macrophage cytosol occurs within 30 min of internalization (Myers *et al.*, 2003). Therefore, characterization of *Lm* vacuoles during the first 30 min after infection should reveal essential features of *Lm* survival in macrophages.

The extent to which *Lm* vacuoles interact with the endocytic pathway of macrophages may be important for *Lm* pathogenesis. Modification of vacuole maturation, particularly inhibition of fusion with lysosomes, is a common strategy among intracellular pathogens such as *Mycobacterium tuberculosis* and *Salmonella typhimurium* (Deretic and Fratti, 1999; Hashim *et al.*, 2000). Vacuoles containing live *hly* *Lm* displayed accelerated fusion with early endosomes and delayed fusion with lysosomes, compared with vacuoles containing heat-killed *Lm* (Alvarez-Dominguez *et al.*, 1997). Prolonged maintenance of the

Received 3 June, 2005; revised 19 July, 2005; accepted 20 July, 2005. *For correspondence. E-mail jswan@umich.edu; Tel. (+1) 734 647 6339; Fax (+1) 734 764 3562.

early endosome marker Rab5a and the late endosome marker Rab7 on *Lm* vacuoles may have delayed fusion with lysosomes (Alvarez-Dominguez *et al.*, 1997; Alvarez-Dominguez and Stahl, 1999). Alternatively, there is evidence that activation of Rab5a on *Lm* vacuoles decreases bacterial escape (Prada-Delgado *et al.*, 2005).

In addition to its role in perforating membranes for *Lm* escape into cytosol, LLO could influence the dynamics of *Lm* vacuole maturation. This issue is difficult to address experimentally. The simplest approach of using fluorescence microscopy of fixed cells to colocalize bacteria with markers of endocytic compartments is complicated by several factors. First, and most importantly, present methods for distinguishing vacuolar from cytosolic *Lm* identify cytosolic bacteria by their recruitment of F-actin, a process that occurs long after bacteria escape from the vacuole. By the time cytosolic bacteria can be identified, they are unlikely to still be associated with the vacuolar compartments from which they escaped. Second, the timing of *Lm* escape varies between 15 and 30 min after infection, so there is no one time point to fix cells for analysis. Third, only some of the vacuoles are perforated, while others retain *Lm* and may continue to later stages of vacuole maturation (de Chastellier and Berche, 1994). Because the timing of maturation may vary between those that are lysed and those that are not, the two populations of vacuoles must be distinguished.

Issues of heterogeneity in phagosome maturation dynamics have been addressed using live cell imaging. The progressive interactions between phagosomes containing IgG-coated erythrocytes and endocytic compartments were observed in live cells using yellow fluorescent protein (YFP) chimeras of endocytic markers (Henry *et al.*, 2004). However, applying this technology to study *Lm* vacuole maturation still requires a method to mark *Lm* when they have gained access to cytosol but not yet shed their vacuolar membranes.

Here we describe a new indicator of *Lm* escape that uses a YFP chimera of the cell wall-binding domain (YFP-CBD) of the *Lm* phage endolysin Ply118 (Loessner *et al.*, 2002). Expression of YFP-CBD within the macrophage cytosol identified cytosolic bacteria shortly after escape. Methods for classification of endocytic compartments were used in conjunction with YFP-CBD to distinguish behaviours of subpopulations of bacteria inside macrophages.

We analysed the progression of *Lm* vacuoles through the endocytic pathway and the escape of *Lm* to the cytosol. RAW 264.7 macrophages expressed YFP-CBD along with one of several cyan fluorescent protein (CFP)-labelled chimeras of endocytic pathway markers. Live cell imaging of macrophages infected with wild-type *Lm* identified recently perforated vacuoles as those containing both CFP-labelled membrane markers and YFP-CBD-

positive bacteria. Employing YFP-CBD as an early indicator of escape not only revealed differences in the maturation of *Lm* vacuole subpopulations, but also identified the compartments permissive to *Lm* escape. Internalized *Lm* did not occupy Rab5a-positive compartments, but instead moved directly into late endosomal compartments. Vacuoles containing wild-type *Lm* delayed fusion with lysosome-associated membrane protein-1 (LAMP1)-positive lysosomes, relative to those containing *hly Lm*. This delay resulted in perforation of Rab7-positive, phosphatidylinositol 3-phosphate [PI(3)P]-positive, LAMP1-negative vacuoles. Although wild-type *Lm* perforated their vacuoles before fusion with LAMP1-positive lysosomes, *Lm* expressing LLO under the control of an inducible promoter [inducible LLO (iLLO)] perforated LAMP1-positive compartments, although very inefficiently. Thus, the LLO-dependent delay in vacuolar maturation facilitates *Lm* escape by increasing the duration of *Lm* residence in penetrable compartments.

Results

*YFP-CBD was an indicator of *Lm* vacuole escape*

The cell wall-binding domain (CBD) from the *Lm* phage endolysin Ply118, which binds to a carbohydrate ligand in *Lm* cell walls with high affinity (Loessner *et al.*, 2002), was developed into a probe for *Lm* escape to the cytosol. Green fluorescent protein (GFP)-tagged CBD could label both wild-type and *hly Lm* when purified and mixed with bacteria in solution (Fig. 1A and B). The CBD was cloned into a mammalian expression vector containing YFP. YFP-CBD expressed in macrophages was present in the cytosol and the nucleus (Fig. 1C and D). To verify that YFP-CBD could be used as an indicator of *Lm* vacuole escape, macrophages expressing YFP-CBD were infected with wild-type, fluorescent *Lm*. Phase-contrast and fluorescence images of infected cells were acquired 10 and 30 min after infection. YFP-CBD expressed inside infected macrophages did not label vacuolar *Lm* shortly after infection (Fig. 1C). However, by 30 min after infection, bacteria decorated with YFP-CBD could be detected (Fig. 1D). Bacteria that appeared to be in the macrophage cytosol were brightly labelled with YFP-CBD, while bacteria within vacuoles were not. To verify that YFP-CBD was a marker of cytosolic *Lm*, the actin polymerization by YFP-CBD-positive *Lm* was measured in cells expressing both YFP-CBD and CFP-actin. YFP-CBD-positive *Lm* labelled with CFP-actin 90 min after infection (Fig. 1E).

The timing of YFP-CBD acquisition by cytosolic bacteria was compared with the timing for F-actin recruitment. While Texas Red (TR)-phalloidin labelled wild-type bacteria 45 min after infection, YFP-CBD-positive bacteria were detected as early as 15 min after infection (Fig. 2). Mutant

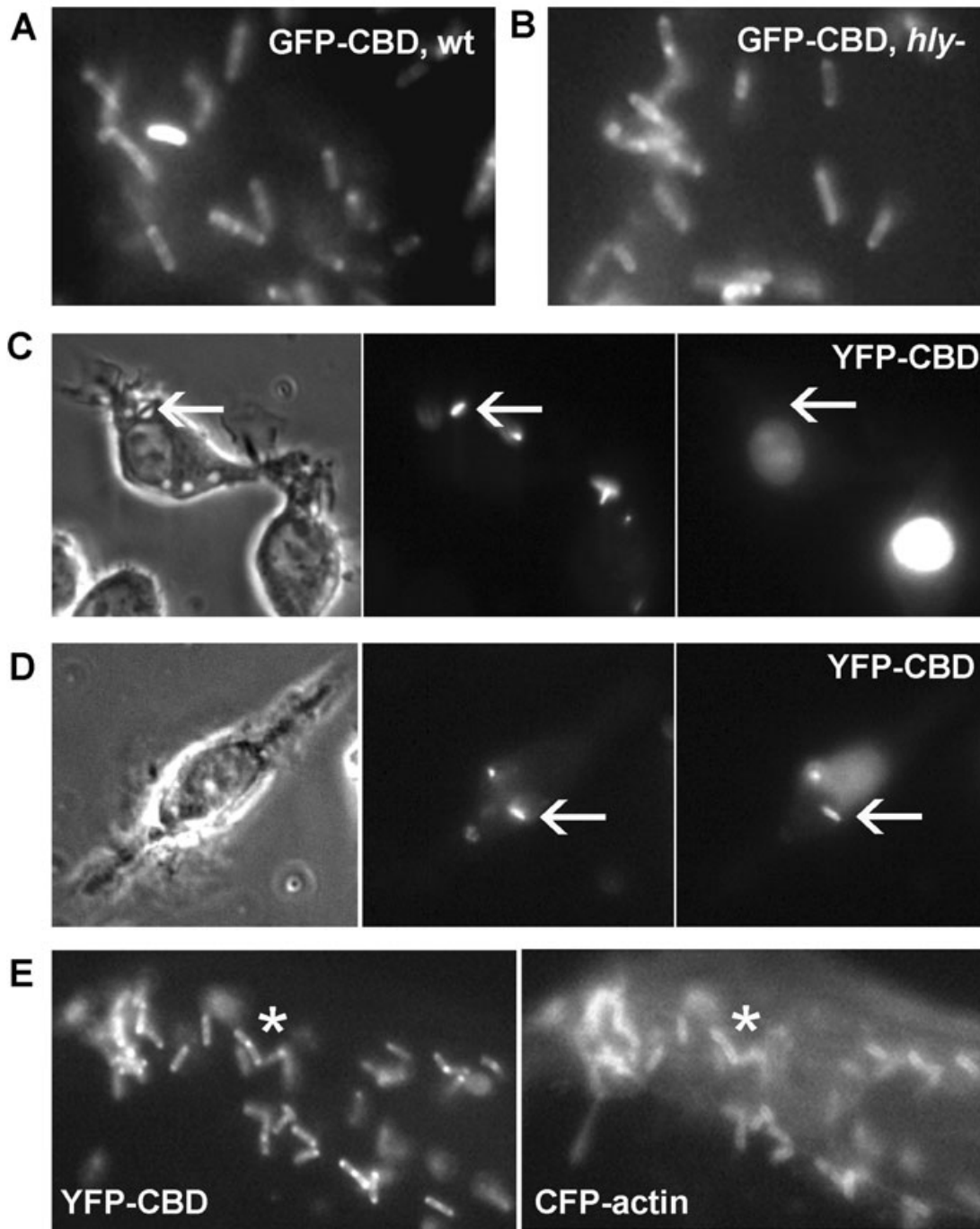


Fig. 1. YFP-CBD as a marker of *Lm* delivery into cytosol.

A and B. Epifluorescence images of (A) wild-type *Lm* and (B) *hly* *Lm* decorated with HGFP-CBD after incubation with the purified fluorescent protein.

C and D. Phase-contrast (left), SNARF-labelled *Lm* (middle) and YFP-CBD fluorescence (right) images. (C) Cells viewed at 10 min after infection contained bacteria in phase-bright vacuoles (arrows) which were not labelled with YFP-CBD. (D) Cells viewed 60 min after infection showed some bacteria labelled with YFP-CBD (arrows).

E. YFP fluorescence image of a RAW 264.7 macrophage showing YFP-CBD-positive cytosolic *Lm* (left) with corresponding labelling by CFP-actin (asterisks).

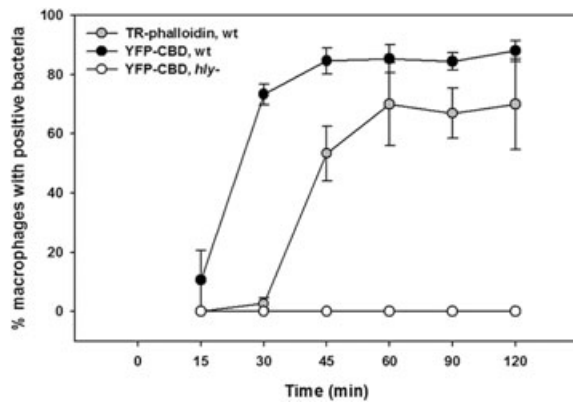


Fig. 2. YFP-CBD marked cytosolic *Lm* within 15 min of infection. Macrophages were infected with wild-type or *hly* *Lm* for 3 min and washed, resulting in <1 bacterium per macrophage. Infected cells were incubated further and fixed at the indicated time points. Bacteria were identified by DAPI staining; cytosolic bacteria were identified by their labelling with either YFP-CBD or TR-phalloidin. At each time point >200 infected cells were scored for the presence of YFP-CBD or TR-phalloidin. YFP-CBD labelled wild-type *Lm* (black circles) between 15 and 30 min, while TR-phalloidin stained wild-type *Lm* (grey circles) 45–120 min after infection. YFP-CBD did not decorate *hly* *Lm* (open circles) at any time. Each data point represents the mean \pm standard error of the mean (SEM) of four experiments.

hly *Lm* never labelled with YFP-CBD, consistent with earlier studies showing that these bacteria do not gain access to macrophage cytosol (Jones and Portnoy, 1994). This time-course experiment demonstrated that YFP-CBD provided a more direct and timely assay for *Lm* vacuole perforation and escape than actin nucleation.

Membrane marker localization to compartments lysed by *Lm*

YFP-CBD was used in conjunction with fluorescent markers of the endocytic pathway to identify the compartments

perforated by *Lm*. The endocytic markers included CFP-Rab5a, CFP-Rab7, LAMP1-CFP and CFP-2xFYVE, which binds to PI(3)P (Gillooly *et al.*, 2000; Stenmark *et al.*, 2002). The overexpression of these CFP chimeras did not alter *Lm* vacuole maturation and escape. The rate of wild-type *Lm* exposure to YFP-CBD was similar in macrophages expressing CFP chimeras or untagged CFP (data not shown). Macrophages were co-transfected with YFP-CBD and one of the CFP-tagged markers of endocytic compartments. Cells were infected for 3 min with wild-type *Lm*, washed free of extracellular bacteria, then phase-contrast, YFP and CFP images of infected cells were taken at regular intervals (Fig. 3). Within 5 min of infection, intravacuolar bacteria were evident as phase-dense rods inside phase-bright vacuoles (Fig. 3A). The bacteria were present in a phase-bright vacuole between 5 and 17 min, after which the vacuole became phase-dark. The phase-bright to phase-dark transition was taken to indicate vacuole perforation. The endocytic compartment in which the bacteria resided was identified by CFP-Rab7 labelling (Fig. 3B). Coincident with the phase-contrast transition, *Lm* were decorated with YFP-CBD (Fig. 3C). Bacteria remained associated with the CFP-Rab7-positive vacuole subsequent to vacuole lysis, as indicated by YFP-CBD (Fig. 3B and C).

The presence of *Lm* in endocytic compartments during the acquisition of YFP-CBD labelling allowed identification of the compartments lysed by *Lm*. Endosomal marker recruitment was quantified by measuring the average CFP fluorescence intensity in a small region including the bacterium (I_p) and dividing it by the average CFP fluorescence intensity of the entire cell (I_c). When the intensity of the phagosome (I_p) equalled the intensity of the cell (I_c) (i.e. $I_p/I_c = 1.0$), the marker was considered not to be enriched on the phagosome. Control macrophages expressing untagged CFP consistently showed I_p/I_c values of 1.0

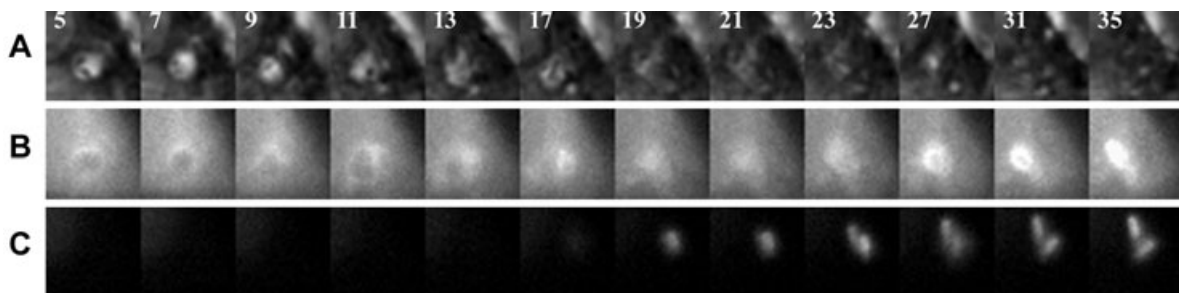


Fig. 3. YFP-CBD allowed identification of compartments lysed by *Lm*. Macrophages were co-transfected with YFP-CBD and CFP-Rab7. Cells were infected with wild-type *Lm*, then phase-contrast, YFP and CFP images of infected cells were taken at 2 min intervals. Each column contains component images of one time point, indicated in (A) as the time, in minutes, after the start of infection. A. Phase-contrast images show two bacteria in a phase-bright vacuole between 5 and 17 min, after which the vacuole became phase-dark. B. CFP-Rab7 labelling of this vacuole illustrated that the vacuole collapsed after 17 min, but fluorescence persisted. CFP fluorescence appeared to increase over time due to movement of the vacuole within the focal plane. C. Coincident with collapse of the vacuole, the bacteria acquired YFP-CBD. From these images it was apparent that bacteria were present in a Rab7-positive compartment during escape to the cytosol.

(Fig. 4A). I_p/I_c values for *Lm* vacuoles significantly greater than 1.0 signified localization of a CFP chimera to the phagosome. Coincident measurement of YFP-CBD recruitment to bacteria allowed discrimination of CFP chimera recruitment to vacuoles perforated by *Lm* (CBD-positive, or CBD+) and intact vacuoles containing CBD-negative (CBD-) *Lm*.

Lm lysed compartments labelled with CFP-Rab7 or CFP-2xFYVE

Wild-type and *hly* *Lm* were present in vacuoles labelled with CFP- or YFP-Rab7 between 5 and 30 min after infection (Fig. 4B and C). The I_p/I_c ratios for vacuoles containing *hly* *Lm* were approximately 1.5 from 5 to 30 min after infection (Fig. 4B). Intact vacuoles containing wild-type *Lm* (CBD-negative) displayed I_p/I_c ratios of 1.5–2.2 (Fig. 4C). The levels of Rab7 on both intact wild-type and *hly* *Lm* vacuoles remained relatively constant. All *Lm* vacuoles observed were labelled with YFP- or CFP-Rab7 at each time point. YFP-CBD-positive wild-type *Lm* were detectable between 15 and 30 min after infection (Fig. 2). I_p/I_c of YFP-CBD-positive bacteria were ~1.5 at 15–20 min after infection, after which the ratio decreased to 1 (Fig. 4D). The high I_p/I_c for CFP-Rab7 when bacteria began to acquire YFP-CBD indicated lysis of Rab7-positive vacuoles by wild-type *Lm*. The colocalization of CFP-Rab7 with YFP-CBD decreased at 25–30 min after infection, possibly due to displacement of the bacteria from their lysed vacuoles.

PI(3)P was recognized by YFP- or CFP-tagged tandem FYVE domains (YFP- or CFP-2xFYVE) (Gillooly *et al.*, 2000; Stenmark *et al.*, 2002). YFP-2xFYVE labelled *hly* *Lm* vacuoles at 5–30 min after infection (Fig. 5A). The marker was also present on intact (CBD-negative) wild-type *Lm* vacuoles over the same time period (Fig. 5B). All *Lm* vacuoles were positive for YFP- or CFP-2xFYVE. CFP-2xFYVE localized to CBD-positive bacteria at 15–20 min after infection, then decreased (Fig. 5C). The colocalization of CFP-2xFYVE and YFP-CBD at 15–20 min indicated the presence of PI(3)P on vacuoles perforated by wild-type bacteria.

CFP-Rab5a was absent from *Lm* vacuoles

Neither YFP-Rab5a nor CFP-Rab5a localized to *Lm* vacuoles from 5 to 30 min. The I_p/I_c ratios in cells expressing YFP- or CFP-Rab5a were near to 1 from 5 to 30 min after infection, indicating absence of this marker from *Lm* vacuoles (Fig. 6A and B). CFP-Rab5a was also not present on vacuoles containing CBD-positive *Lm* (Fig. 6C).

It was possible that YFP-Rab5a was present on *Lm* vacuoles transiently and before the earliest time point measured. To test this possibility, phase-contrast and YFP

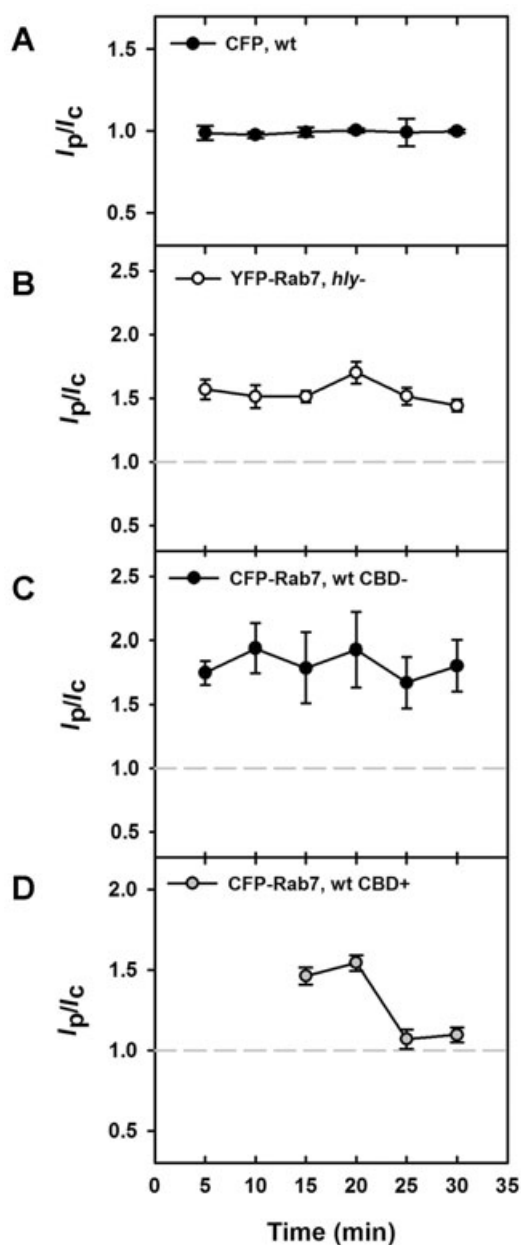


Fig. 4. *Lm* lysed compartments labelled with Rab7. The average fluorescence intensity of the phagosome (I_p) was divided by the average fluorescence intensity of the entire cell (I_c) to produce the cell-normalized phagosome fluorescence (I_p/I_c). Each symbol represents the mean values of >45 vacuoles measured in multiple experiments.

A. I_p/I_c ratios for *Lm* vacuoles in macrophages expressing CFP were near 1.0 from 5 to 30 min. These values were compared as a negative control to all further experiments (grey dotted line in subsequent panels).

B and C. (B) *hly* *Lm* and (C) YFP-CBD-negative, wild-type *Lm* resided in Rab7-positive vacuoles between 5 and 30 min after infection, as indicated by I_p/I_c values significantly higher than those in cells expressing CFP ($P < 0.01$). One hundred per cent of *Lm* vacuoles were Rab7-positive.

D. YFP-CBD-positive, wild-type *Lm* displayed I_p/I_c ratios greater than 1.5 for CFP-Rab7 from 15 to 20 min, demonstrating that *Lm* lysed compartments labelled with CFP-Rab7.

The bars indicate SEM.

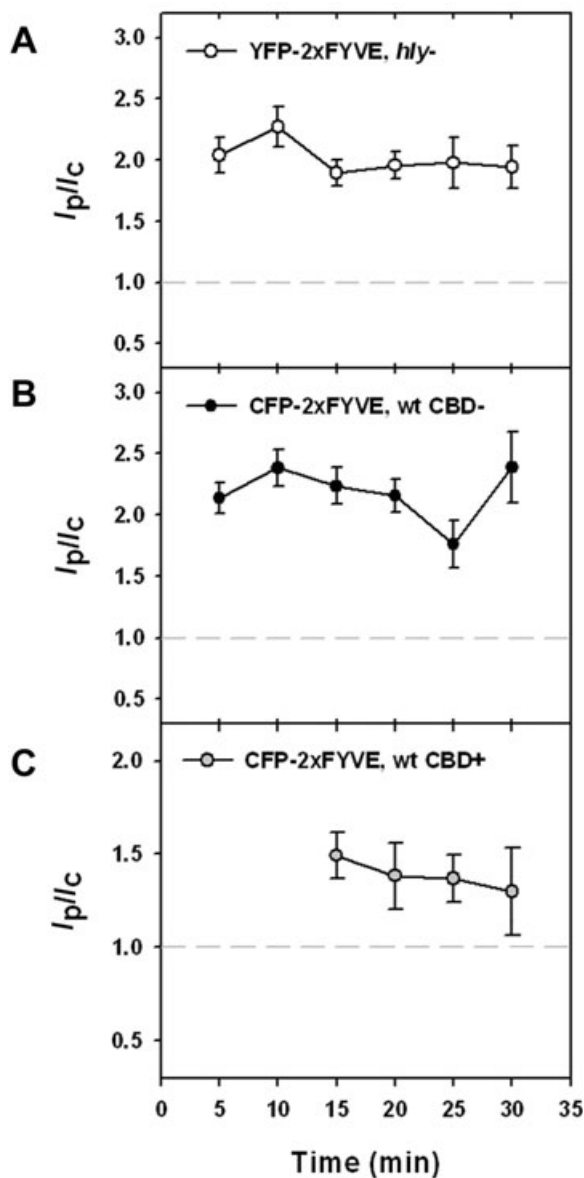


Fig. 5. PI(3)P on vacuoles lysed by *Lm*. A and B. YFP- or CFP-2xFYVE-labelled vacuoles containing (A) *hly* *Lm* and (B) YFP-CBD-negative, wild-type *Lm* at 5–30 min. One hundred per cent of *Lm* vacuoles were 2xFYVE-positive. C. CFP-2xFYVE and YFP-CBD colocalized 15–20 min after infection, signifying the presence of PI(3)P on vacuoles perforated by wild-type bacteria. At each time point >45 vacuoles were measured. The bars indicate SEM.

images were collected during internalization of *Lm* into YFP-Rab5a-expressing RAW 264.7 or J774 macrophages. YFP-Rab5a was not present on wild-type *Lm* vacuoles during internalization or the first few minutes subsequent to vacuole formation in either cell line (Fig. 7A).

YFP-Rab5a localized to newly formed phagosomes containing IgG-opsonized erythrocytes in RAW 264.7 macrophages (Henry *et al.*, 2004). Thus, the stimulation

of Fc receptors by *Lm* might localize YFP-Rab5a to *Lm* vacuoles. The internalization of IgG-opsonized *Lm* was observed in YFP-Rab5a-expressing RAW 264.7 macrophages. YFP-Rab5a did localize transiently to vacuoles containing IgG-opsonized *Lm* (Fig. 7A and B).

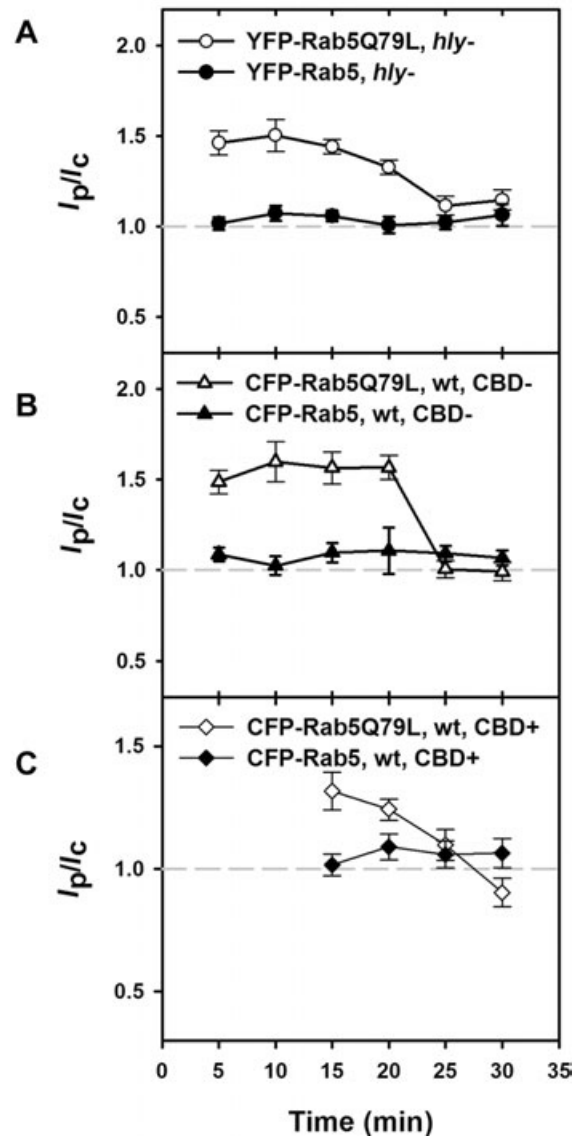


Fig. 6. Rab5 did not label *Lm* vacuoles, but localization of Rab5Q79L to *Lm* vacuoles did not prevent escape.

A. While YFP-Rab5a did not localize to vacuoles containing *hly* *Lm* (closed circles), YFP-Rab5Q79L was present from 5 to 20 min (open circles).

B. CFP-Rab5Q79L localized to CBD-negative, wild-type *Lm* vacuoles from 5 to 20 min (open triangles), but CFP-Rab5a did not (closed triangles).

C. CFP-Rab5a was not associated with YFP-CBD-positive *Lm* at any time point measured (closed diamonds). CFP-Rab5Q79L associated with CBD-positive *Lm* at 15–20 min (open diamonds), demonstrating that *Lm* could lyse vacuoles labelled with Rab5Q79L. At each time point >45 vacuoles were measured.

The bars indicate SEM.

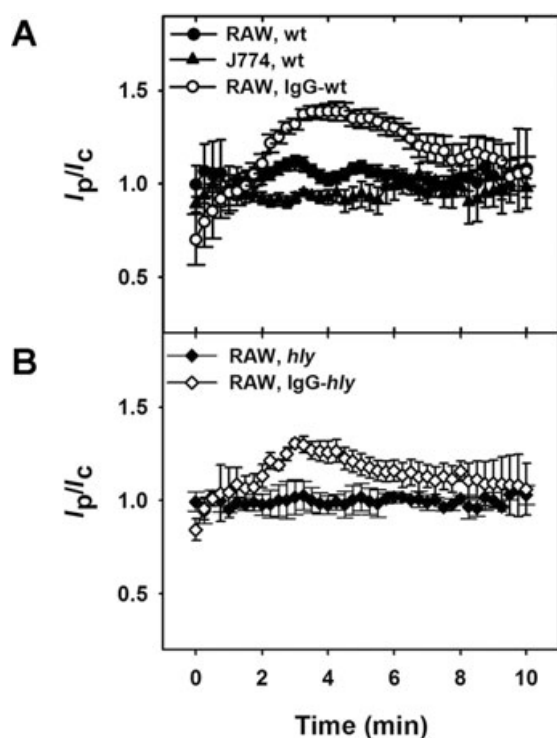


Fig. 7. Rab5a was not present on *Lm* vacuoles, but did localize transiently to vacuoles containing IgG-opsonized *Lm*.

A. The internalization of wild-type *Lm* was observed in RAW 264.7 (closed circles) or J774 macrophages (closed triangles). YFP-Rab5a was not associated with wild-type *Lm* vacuoles during internalization or the first 5 min subsequent to internalization. YFP-Rab5a associated transiently with vacuoles during entry of IgG-opsonized *Lm* into RAW 264.7 macrophages (open circles).

B. YFP-Rab5a did not associate with vacuoles containing *hly* *Lm* (closed diamonds), but did associate transiently with vacuoles containing IgG-opsonized, *hly* *Lm* (open diamonds). The data were aligned by the timing of phase-bright vacuole formation, which was set at 3 min.

At each time point >15 vacuoles were measured. The bars indicate SEM.

Rab5Q79L localization to *Lm* vacuoles did not inhibit escape

The absence of Rab5a from *Lm* vacuoles could have facilitated *Lm* escape. To determine whether forced localization of Rab5a to vacuoles could inhibit *Lm* escape, we analysed *Lm* vacuoles in macrophages expressing CFP-Rab5Q79L. This mutant form of CFP-Rab5a is locked in the GTP-bound state and is recruited to membranes (Roberts *et al.*, 2000). YFP- or CFP-Rab5Q79L was present on large endocytic vesicles within macrophages, and localized to vacuoles containing *hly* and wild-type *Lm* (Fig. 6A and B). I_p/I_c ratios were significantly greater than 1.0 from 5 to 20 min after infection. The decline in I_p/I_c values at 25 min may be due to fusion of vacuoles with late endosomes and lysosomes. YFP-CBD-positive bacteria were associated with CFP-Rab5Q79L-labelled vac-

uoles by wild-type *Lm* (Fig. 6C). Moreover, expression of CFP-Rab5aQ79L did not affect the rate of *Lm* exposure to YFP-CBD (data not shown). Thus, localization of CFP-Rab5Q79L to *Lm* vacuoles did not inhibit escape of bacteria to the cytosol.

Wild-type *Lm* perforated vacuoles before fusion with LAMP1-positive compartments

Vacuoles containing *hly* bacteria acquired LAMP1-YFP from 15 to 25 min after infection, as indicated by I_p/I_c values near 1.5 (Fig. 8A). The acquisition of LAMP1-CFP by vacuoles containing wild-type *Lm* was delayed relative to *hly* vacuoles. Intact vacuoles containing wild-type *Lm*

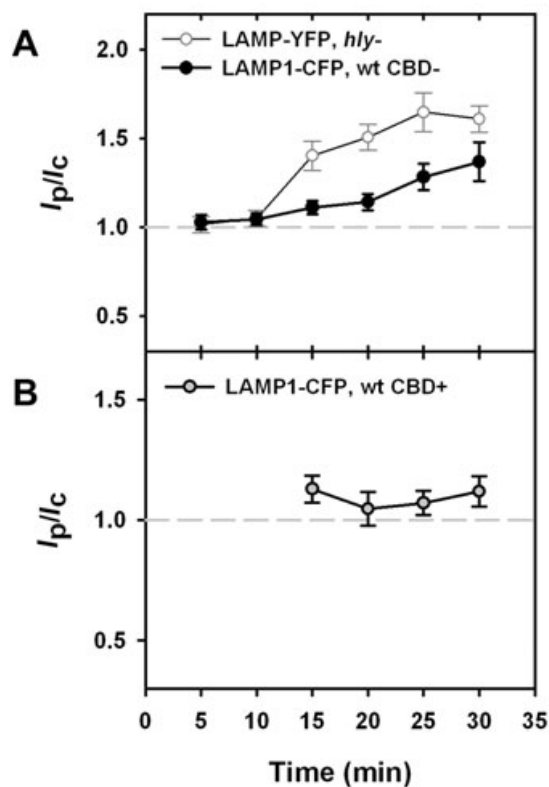


Fig. 8. Wild-type *Lm* phagosomes showed delayed acquisition of LAMP1-CFP.

A. Vacuoles containing *hly* bacteria (open circles) acquired LAMP1-YFP from 15 to 30 min after infection, as indicated by I_p/I_c values near 1.5. Ninety per cent of vacuoles were LAMP1-positive at 15 min, and 100% of vacuoles were LAMP1-positive at 30 min. The acquisition of LAMP1-CFP by vacuoles containing CBD-negative wild-type *Lm* was delayed relative to *hly* phagosomes. I_p/I_c did not reach a value significantly higher than 1.0 until 25 min ($P < 0.01$). Three per cent of vacuoles containing CBD-negative wild-type *Lm* were LAMP1-positive at 15 min, and 96% were LAMP1-positive at 30 min.

B. Lack of colocalization of LAMP1-CFP with YFP-CBD indicated that *Lm* escaped to the cytosol before association with LAMP1-CFP labelled lysosomes. While I_p/I_c ratios for CBD-negative, wild-type *Lm* were high from 25 to 30 min, I_p/I_c ratios for CBD-positive wild-type *Lm* remained low ($P < 0.01$).

At each time point >45 vacuoles were measured. The bars indicate SEM.

(CBD-negative) did not show LAMP1-CFP labelling until 25 min (Fig. 8A), indicating that wild-type *Lm* delayed fusion with LAMP1-CFP-positive compartments. Furthermore, LAMP1-CFP did not colocalize with YFP-CBD even at later time points (Fig. 8B), indicating that *Lm* perforated its vacuole before merging with LAMP1-labelled compartments. Thus, even before it created perforations large enough to admit YFP-CBD, LLO delayed *Lm* vacuole maturation.

Inefficient perforation of LAMP1-positive compartments

It was possible that the normal timing of LLO activity caused perforation of the vacuoles before fusion with LAMP1-positive compartments, but that *Lm* was nonetheless capable of perforating LAMP1-positive compartments. To examine the efficiency of perforation at later stages of *Lm* vacuole maturation, the timing of LLO production was manipulated experimentally by placing transcriptional control of LLO under an isopropyl- β -D-thiogalactopyranoside (IPTG)-inducible promoter and incorporating the construct into the chromosome of *hly* *Lm* (Dancz *et al.*, 2002). In the absence of IPTG, the iLLO *Lm* were trapped in vacuoles and could not escape to the cytosol (Fig. 9A and C). Addition of

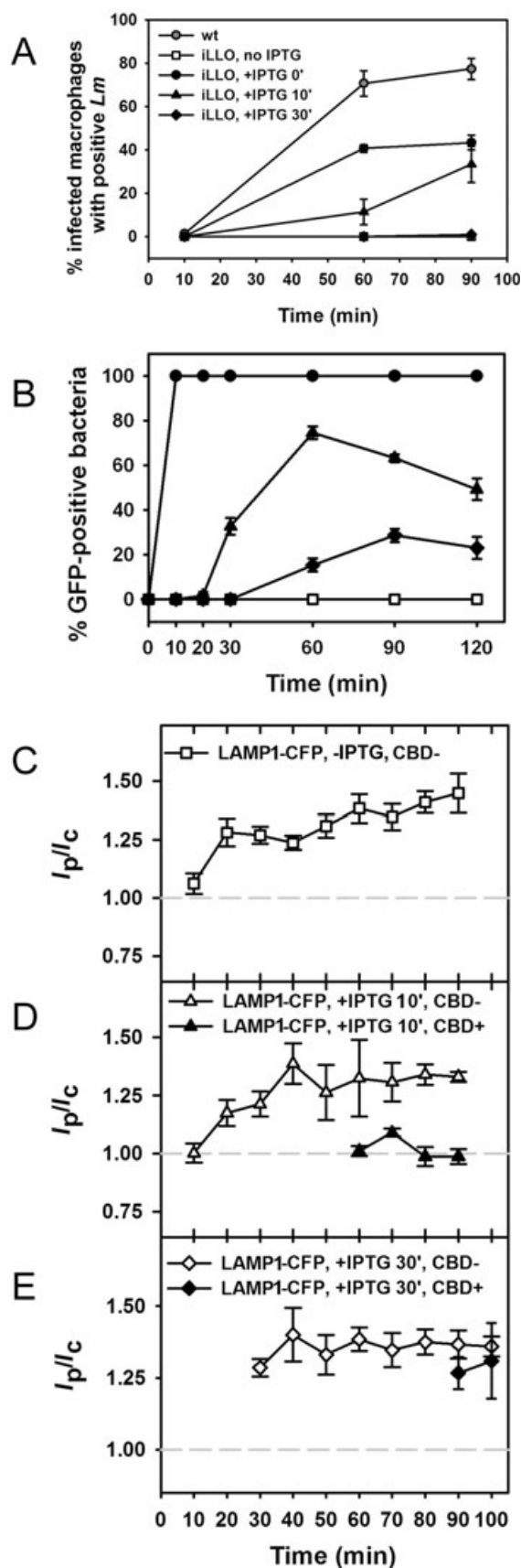
Fig. 9. Perforation of LAMP1-positive compartments by LLO was inefficient.

A. Macrophages expressing YFP-CBD were infected with wild-type or iLLO *Lm* to produce <1 bacterium per macrophage and were fixed at the indicated time points. Infected cells were identified by DAPI staining and cytosolic bacteria were identified by YFP-CBD labelling. YFP-CBD labelled wild-type *Lm* (grey circles) by 60 min. Escape of iLLO *Lm* treated with 10 mM IPTG before infection (IPTG 0', black circles) was reduced relative to wild type. iLLO *Lm* treated with IPTG at 10 min after infection (IPTG 10', triangles) were present in the cytosol at 60 min. iLLO *Lm* treated with IPTG at 30 min (IPTG 30', diamonds) did not become CBD-labelled until 90 min, at which point ~0.5% were YFP-CBD-positive. In the absence of IPTG (open squares, partially obscured by IPTG 30' data), no *Lm* were CBD-labelled. At each time point >100 infected cells were scored for the presence of YFP-CBD. Each data point represents the mean \pm SEM of two experiments.

B. Overnight cultures of iGFP *Lm* or macrophages infected with iGFP *Lm* were fixed at the indicated time points. Intracellular bacteria were identified by DAPI staining and GFP-producing bacteria were identified by indirect immunofluorescence. iGFP *Lm* treated with IPTG in broth (black circles) stained positive for GFP by 10 min. iGFP *Lm* treated with IPTG at 10 min after infection stained positive for GFP from 30 to 120 min (black triangles), whereas iGFP *Lm* treated with IPTG at 30 min stained positive for GFP from 60 to 120 min (black diamonds). iGFP *Lm* did not stain positive for GFP in the absence of IPTG treatment (open squares). At each time point 100 bacteria were scored for Alexa Fluor 594 staining. Each data point represents the mean \pm SEM of two experiments.

C. Uninduced iLLO *Lm* acquired LAMP1-CFP by 20 min after infection, but did not decorate with YFP-CBD at any time (open squares). D. After treatment with IPTG at 10 min after infection, iLLO *Lm* escaped from LAMP1-CFP-negative compartments at 60–90 min (closed triangles). Many CBD-negative vacuoles acquired LAMP1-CFP as early as 20 min (open triangles).

E. In cells treated with IPTG at 30 min after infection, iLLO *Lm* perforated LAMP1-CFP-positive vacuoles at 90–100 min (closed diamonds).



10 mM IPTG to iLLO *Lm* immediately before infection yielded less efficient vacuole perforation than wild-type *Lm*, but similar kinetics (Fig. 9A). Addition of IPTG to macrophages at 10 min after infection resulted in delayed perforation, and induction of LLO at 30 min resulted in greatly reduced and delayed perforation. Approximately 0.5% iLLO *Lm* were CBD-positive at 90 min (Fig. 9A).

The small number of CBD-positive iLLO *Lm* observed after treatment of macrophages with IPTG at 30 min (Fig. 9A) may have resulted from a low percentage of LLO-producing *Lm*, due either to limited access of IPTG to *Lm* vacuoles or to decreased viability of *Lm* inside those vacuoles. Attempts to detect LLO in vacuoles by immunofluorescence were not successful. Instead, the efficiency of protein synthesis induced by IPTG was inferred using *hly Lm* that produce GFP [inducible GFP (iGFP) *Lm*] using the same IPTG-inducible promoter as found in the iLLO strain. GFP production was detected by immunofluorescence staining with an anti-GFP antibody, as GFP fluorescence may not be observed until 90 min to 4 h after protein synthesis (Zimmer, 2002). iGFP *Lm* treated with IPTG in broth stained positive for GFP within 10 min after adding IPTG (Fig. 9B). iGFP *Lm* in macrophages treated with IPTG at 10 min after infection began to stain positive for GFP by 30 min (Fig. 9B). Treatment of infected macrophages with IPTG at 30 min led to GFP synthesis in 15–29% of bacteria (Fig. 9B). The reduction in the number of GFP-positive bacteria at 120 min may have been caused by degradation of bacteria within vacuoles. Comparison of the 90 min time points in Fig. 9A and B shows that prolonged *Lm* residence in vacuoles diminished its ability to escape more than its ability to respond to IPTG. Thus, LLO perforated early endocytic compartments more efficiently than late-stage endocytic compartments.

We next determined whether the late-stage vacuoles perforated by iLLO *Lm* were LAMP1-positive. In the absence of IPTG, vacuoles containing iLLO *Lm* acquired LAMP1-CFP by 20 min (Fig. 9C). Although many iLLO *Lm* resided in LAMP1-positive vacuoles at 60 min, some bacteria were present in LAMP1-negative compartments. Only the iLLO *Lm* in LAMP1-negative vacuoles became CBD-positive (Fig. 9D). Induction of LLO at 30 min, a delay that should have allowed all of the bacteria to reach LAMP1-positive compartments, showed a very limited level of escape; 0.5% of the intracellular bacteria were CBD-positive at 90 min (Fig. 9A). However, those few CBD-positive iLLO *Lm* had perforated LAMP1-CFP-positive vacuoles (Fig. 9E). Thus, LAMP1-positive vacuoles may be perforated by *Lm*, but that perforation is very inefficient. The ability of *Lm* to delay arrival into LAMP1-positive compartments therefore facilitated *Lm* escape.

Discussion

A new method for detecting *Lm* escape into the cytosol allowed novel questions regarding the contributions of LLO to *Lm* vacuole maturation to be addressed. Decoration of *Lm* by cytosolic YFP-CBD occurred while bacteria were still enveloped by their perforated vacuoles. CFP-labelled membrane markers characterized those newly lysed vacuoles as late endosomal, LAMP1-negative organelles. The coincident localization of membrane markers and CBD was transient; by 25 min after infection, YFP-CBD-positive bacteria were no longer associated with CFP-labelled vacuolar membranes (Figs 4D and 5C). Recently lysed vacuoles could not be identified using F-actin accumulation by *Lm* as a measure of escape, as TR-phalloidin staining of cytosolic bacteria occurred no sooner than 45 min after infection (Fig. 2). As an early indicator of escape, YFP-CBD allowed discrimination of the different maturation pathways of *Lm* vacuole subpopulations. Vacuoles that were perforated (CBD-positive) matured differently from intact vacuoles (CBD-negative). Vacuoles containing CBD-negative wild-type or *hly Lm* acquired LAMP1-CFP, but vacuoles containing CBD-positive *Lm* did not (Fig. 8). The measurement of *Lm* escape with YFP-CBD will allow further analyses of *Lm* vacuole dynamics.

Localization of YFP-CBD-positive bacteria in PI(3)P-, Rab7-positive vacuoles classified the compartment of escape as a late endosome. This Rab5a-negative, LAMP1-negative, PI(3)P-positive, Rab7-positive compartment persisted from internalization until vacuole perforation (Figs 4 and 5). In contrast, in phagosomes containing opsonized erythrocytes the analogous stage of maturation was more transient (Henry *et al.*, 2004). The prolongation of the PI(3)P-, Rab7-positive stage of *Lm* vacuole maturation facilitated *Lm* escape. The pH of late endosomal vacuoles is optimal for LLO activity, as the cytolysin is most active between pH 5.5 and 6.0 (Portnoy *et al.*, 1992; Conte *et al.*, 1996; Beauregard *et al.*, 1997).

Absence of the early endosome marker YFP- or CFP-Rab5a from *Lm* vacuoles in both RAW 264.7 and J774 macrophages (Figs 6 and 7) is at odds with earlier studies that indicated roles for Rab5a in *Lm* vacuole maturation in J774 macrophages (Alvarez-Dominguez and Stahl, 1999; Prada-Delgado *et al.*, 2001). However, neither study illustrated the localization of Rab5a to *Lm* vacuoles. Rab5a may be excluded from *Lm* vacuoles due to an absence of GTP-exchange mechanisms necessary for its association with *Lm* vacuole membranes (Prada-Delgado *et al.*, 2005). The overexpression of Rab5Q79L, which is locked in the GTP-bound state, bypassed this step and Rab5Q79L localized to *Lm* vacuoles (Fig. 6). *Lm* may actively inhibit Rab5 GTP exchange, or *Lm* entry into macrophages may not involve activation of Rab5 guanine

nucleotide exchange factors (GEFs). The localization of Rab5a to *Lm* vacuoles upon stimulation of Fc receptors by IgG-opsonized *Lm* (Fig. 7) indicated that *Lm* did not block Rab5 GTP exchange. Rather, the receptors normally stimulated during *Lm* phagocytosis by macrophages may not activate Rab5 GEFs.

The implications of Rab5a exclusion from *Lm* vacuoles are not known. The absence of Rab5a from *Lm* vacuoles may enhance *Lm* survival within macrophages. Overexpression of Rab5a in J774 macrophages enhanced intracellular killing of *Lm* (Prada-Delgado *et al.*, 2001). One method by which macrophages can control *Lm* infection is through retention of bacteria within vacuoles (Portnoy *et al.*, 2002). Our results demonstrated that overexpression of CFP-Rab5a or CFP-Rab5Q79L did not prevent *Lm* escape in RAW 264.7 macrophages (Fig. 6C). Furthermore, the efficiency of escape in cells expressing YFP-Rab5a, YFP-Rab5Q79L or YFP-Rab5S34N (a dominant-negative Rab5 mutant) was similar to that in untransfected control cells (data not shown). Alternatively, Rab5a may enhance macrophage killing of *Lm* through a mechanism other than inhibition of vacuolar escape (Prada-Delgado *et al.*, 2001).

Escape of *Lm* to the cytosol was facilitated by delayed fusion of *Lm* vacuoles with LAMP1-positive lysosomes. Wild-type *Lm* vacuoles fused more slowly than *hly* *Lm* vacuoles with LAMP1-positive compartments (Fig. 8A), allowing wild-type *Lm* to escape from vacuoles before acquisition of LAMP-1 (Fig. 8B). Vacuoles containing wild-type *Lm* fused more slowly with lysosomes than *hly* *Lm* vacuoles, further indicating that LLO delays vacuole maturation (data not shown). The cholesterol-dependent cytolysin streptolysin O prevented internalization of group A *Streptococcus* into lysosomes in epithelial cells, indicating that evasion of lysosomal killing may be a common function among cholesterol-dependent cytolysins (Hakansson *et al.*, 2005).

Listeriolysin O perforated late-stage vacuoles inefficiently. Although *Lm* containing LLO under the control of an IPTG-inducible promoter could perforate LAMP1-positive compartments 90 min after infection (Fig. 9E), very few did so (Fig. 9A). Based on the responsiveness of iGFP to IPTG, it appeared that induction of LLO synthesis did not occur within all iLLO *Lm* vacuoles. However, this factor cannot account entirely for the inefficient escape of iLLO *Lm* at late time points. Thus, LAMP1-positive compartments inhibited vacuolar escape. LAMP-1 is a transmembrane protein, with a large, heavily glycosylated luminal domain (Peters and von Figura, 1994). The barrier created by LAMP-1 and other lysosomal membrane proteins may hinder the insertion of LLO into the phagosomal membrane, thus inhibiting escape. Alternatively, the lysosomal proteases such as cathepsin D could inhibit LLO function (Prada-Delgado *et al.*, 2005), or

vacuoles at late stages may be depleted of cholesterol and therefore less susceptible to cholesterol-dependent LLO. Regardless of the mechanism, it is clear that *Lm* benefits from the LLO-dependent delay of arrival into LAMP1-positive compartments.

How does LLO slow vacuole maturation? The delay was evident even in CBD-negative vacuoles containing wild-type *Lm*; an indication that LLO altered maturation well before vacuolar membranes were perforated enough for YFP-CBD labelling. Before *Lm* vacuole lysis and escape, LLO forms small pores in the vacuole, which cause an elevation of vacuolar pH and a decrease in intravacuolar calcium (L.M. Shaughnessy, A.D. Hoppe, K.A. Christensen and J.A. Swanson, submitted). An acidic pH is necessary for vacuole maturation (Gordon *et al.*, 1980; Mellman *et al.*, 1986; van Weert *et al.*, 1995). Calcium has also been implicated in endosome fusion with lysosomes. Depletion of calcium from endocytic compartments has been shown to block fusion with lysosomes (Peters and Mayer, 1998; Pryor *et al.*, 2000). The release of calcium and protons from the vacuole may account for the LLO-mediated alteration of vacuole maturation.

Listeriolysin O is an extraordinary cytolysin. Its action is largely restricted to vacuoles, with little collateral damage incurred by infected host cells (Glomski *et al.*, 2002). The compartmentalization of LLO activity is necessary for *Lm* virulence (Glomski *et al.*, 2003). *Lm* require the hospitable cytosolic environment of host cells for survival (Portnoy *et al.*, 2002). Escaping before fusion with lysosomes would prevent the contents of perforated lysosomes from spilling into the cytosol, maintaining the habitable cytosolic environment. The ability of LLO to delay *Lm* arrival into LAMP1-positive compartments represents a novel survival mechanism for an intracellular pathogen.

Experimental procedures

Bacteria

Listeria monocytogenes (*Lm*) wild-type strain 10403S, mutant *hly* strain DP-L2161 (gifts of D. Portnoy, University of California, Berkeley, CA), iLLO strain DH-L388 (Dancz *et al.*, 2002) and iGFP strain were maintained on brain–heart infusion (BHI) agar plates. One bacterial colony was added to BHI broth, shaken overnight at room temperature, diluted 1:5 the following morning and shaken at 37°C for 90 min. Bacteria were washed with Ringer's buffer (155 mM NaCl, 5 mM KCl, 2 mM CaCl₂, 1 mM NaH₂PO₄, 10 mM Hepes and 10 mM glucose, pH 7.2) three times before addition to macrophages. For *Lm* opsonization, washed *Lm* were opsonized with 5 µl of Difco *Listeria* O Type 1 Antiserum (Becton, Dickinson and Co., Sparks, MD) for 30 min at 37°C, and then washed once with Ringer's buffer.

Construction of the iGFP *Lm* strain

Plasmid pDH1038 harbouring the *gfpmut2* gene under control of

the constitutive HyperSPO1 promoter (Shen and Higgins, 2005) was digested with *EagI* and *Sall* to remove a promoterless *gfp* containing DNA fragment. The *gfp* DNA fragment was ligated into the inducible expression vector pLIV2 (Higgins *et al.*, 2005) that had been previously digested with *EagI* and *Sall*. The resulting plasmid, pDH1269, containing the *gfpmut2* gene under control of the IPTG-inducible SPAC/*lacOid* promoter (Dancz *et al.*, 2002), was electroporated into *hly Lm* (DP-L2161) to generate an iGFP *Lm* strain (DH-L1271). Electroporation was performed as previously described (Lauer *et al.*, 2002) and resulted in site-specific integration of the iGFP vector within the *tRNA^{Arg}* locus of the *hly Lm* strain.

Cell culture

RAW 264.7 and J774A.1 macrophages were grown in Dulbecco's modified Eagle medium (DMEM, Invitrogen, Carlsbad, CA) supplemented with 10% heat-inactivated fetal bovine serum (FBS, Invitrogen), and 100 unit ml⁻¹ penicillin/streptomycin mixture (Sigma-Aldrich, St Louis, MO) at 37°C with 5% CO₂. During live microscopic observation, the live cells were maintained at 37°C on a heated stage in Ringer's buffer.

YFP and CFP constructs

Polymerase chain reaction (PCR)-amplified coding sequences of Rab5a (provided by Philip Stahl, Washington University, St Louis, MO) and Rab7 (gift from Angela Wandinger-Ness, University of New Mexico, Albuquerque, NM) were subcloned into pEYFP-C1 and pECFP-C1 vectors (Clontech, Palo Alto, CA) to create YFP-Rab5a, CFP-Rab5a, YFP-Rab7 and CFP-Rab7. 2xFYVE, containing two linked FYVE finger domains from hepatocyte growth factor-regulated tyrosine kinase substrate (supplied by Harald Stenmark, Norwegian Radium Hospital, Oslo, Norway), was subcloned into pEYFP-C1 and pECFP-C1 to create YFP-2xFYVE and CFP-2xFYVE. LAMP-1 (provided by Norma Andrews, Yale University School of Medicine, New Haven, CT) was inserted into pEYFP-N1 or pECFP-N1 (Clontech, Palo Alto, CA) to create LAMP1-YFP and LAMP1-CFP. The C-terminal CBD of *Listeria* phage endolysin Ply118 (Loessner *et al.*, 2002) was cloned into pEYFP-C1 to create YFP-CBD. CFP-actin was purchased from Clontech. All constructs were verified by sequencing.

RAW 264.7 cells were transfected with Eugene 6 (Roche, Indianapolis, IN), as per manufacturer's instructions. All DNA used for transfection was prepared with a MaxiPREP kit (Qiagen, Valencia, CA).

His-tagged GFP (HGFP)-CBD was purified and used to label *Lm* as previously described (Loessner *et al.*, 2002).

Phagosomal escape assays

The percentage of bacteria that escaped from vacuoles was determined by modification of a method previously described (Jones and Portnoy, 1994; Myers *et al.*, 2003). Briefly, RAW macrophages were plated on 13 mm diameter circular coverslips, infected with *Lm* [multiplicity of infection (moi) ~1] for 10 min at 37°C in DMEM, 10% FBS (time zero was defined as the time of addition of bacteria), and washed with Ringer's buffer. Infection resulted in <1 bacterium per macrophage. Cells were incubated for an additional 5–80 min, fixed for 15 min and permeabilized.

All permeabilized cells were incubated for 15 min with DAPI (2 µg ml⁻¹, Molecular Probes, Eugene, OR) and non-transfected cells were also incubated with TR-phalloidin (2 U ml⁻¹, Molecular Probes). Cells were washed with PBS and goat serum and mounted on glass slides with Prolong Antifade (Molecular Probes).

For Figs 2 and 7, *Lm* escape was quantified by scoring the number of infected macrophages containing CBD-positive or TR-phalloidin-positive *Lm*. This scoring method corrected for *Lm* replication in the macrophage cytosol at late time points. For each coverslip, 50 macrophages with DAPI-labelled bacteria were scored for colocalization of bacteria with filamentous actin or YFP-CBD. In the remaining figures, escape was quantified by scoring the number of YFP-CBD-positive *Lm*.

For morphological detection of YFP-CBD labelling in macrophages (Fig. 1C and D), *Lm* were labelled for 15 min with 3 µl ml⁻¹ SNARF-1 carboxylic acid, acetate, succinimidyl ester (Molecular Probes) solution in DMSO, then washed three times with Ringer's buffer before infection of YFP-CBD-expressing macrophages (for 3 min at 37°C). Phase-contrast, YFP and RFP (i.e. SNARF1 fluorescence) images were collected at regular intervals. Excitation filters (S492/18×, S580/20×, Chroma Technology) and emission filters (S535/30m, S630/60m, Chroma Technology) were used along with a dichroic mirror (86006bs, Chroma Technology) to separately image YFP and SNARF-1. A phase-contrast image, YFP image (492 excitation, 535 emission) and SNARF-1 image (580 excitation, 630 emission) were taken of YFP-CBD macrophages infected with red-labelled *Lm* (SNARF-1) at different times after infection.

Localization of *Lm* within endocytic compartments

Macrophages were plated on 25 mm circular coverslips (3 × 10⁵ cells per coverslip) overnight, and then placed on a temperature-controlled stage mounted on the inverted fluorescence microscope. Imaging employed two filter wheels, shutters to control light exposure, selective dichroic mirrors for viewing both YFP and CFP (Omega Optical, Brattleboro, VT) and cooled CCD camera (Photometrics). For determination of time-courses for *Lm* vacuole maturation, transfected cells were pulsed with wild-type or *hly Lm* for 3 min (moi ~5), washed four times with Ringer's buffer, and phase-contrast, YFP fluorescence and CFP fluorescence (when applicable) images of infected cells were acquired every 2–5 min for 30 min. When observing bacterial uptake, washed *Lm* were added to transfected cells (moi ~1) and phase-contrast and YFP fluorescence images were collected at 15 s intervals for 10 min.

For experiments with strain DH-L388 (iLLO), macrophages were infected for 5 min with DH-L388 and washed four times with Ringer's buffer. Infected macrophages were treated with 10 mM IPTG at 10 min or 30 min after infection, or left untreated. Phase-contrast, YFP fluorescence and CFP fluorescence images of infected cells were taken every 10 min for 90–100 min.

Primary fluorescence images were background-corrected by subtracting the mean intensity measured from a cell-free region. The dynamics of YFP or CFP chimeras on *Lm* vacuoles were analysed quantitatively by measuring the mean YFP or CFP intensities in a circular region placed over the phagosome (*I_p*), as well the mean intensities within a region drawn around the entire cell (*I_c*). Dividing these values to obtain the phagosome ratio (*I_p/I_c*) allowed for comparison of vacuoles between cells of

varying YFP or CFP chimera expression level. Colocalization of CFP chimeras with YFP-CBD was determined by drawing a region around a bacterium in the phase-contrast image, transferring the region to the CFP chimera and YFP-CBD images, measuring I_p , and then subsequently measuring I_c .

I_p/I_c values for YFP-Rab5a in experiments in which *Lm* uptake was observed were temporally aligned by vacuole formation. This was determined in phase-contrast images by the movement of *Lm* from the phase-dark extracellular environment to the phase-bright vacuolar environment. A sharp rise in grey values surrounding the bacteria marked this transition (Hoppe and Swanson, 2004). Vacuole formation was set to 3 min and all ratio data were aligned by this time point.

I_p/I_c values for all experiments were compared with I_p/I_c values for *Lm* vacuoles in macrophages expressing untagged CFP, a fluorescent marker that did not localize to *Lm* vacuoles. If the I_p/I_c values from cells expressing fluorescently tagged Rab5a, Rab7, 2xFYVE or LAMP-1 were significantly greater than I_p/I_c values from cells expressing CFP, then the marker was considered localized to the phagosome. Significant differences between the data were determined using Student's *t*-test.

Processed images were prepared for presentation using Adobe Photoshop and Adobe Premiere (Adobe Systems, San Jose, CA).

Immunofluorescence staining for GFP synthesis

Macrophages were plated on 13 mm circular coverslips (5×10^4 cells per coverslip) overnight, infected with washed iGFP *Lm* for 5 min, washed with Ringer's buffer and incubated for an additional 5–115 min. Infected macrophages were treated with 10 mM IPTG at 10 min or 30 min after infection, or left untreated. After incubation, cells were fixed for 30 min with 4% paraformaldehyde, 0.05% glutaraldehyde, 20 mM HEPES and 0.2 M sucrose, and permeabilized with PBS, 0.3% Triton. Synthesis of GFP was determined by staining cells with DAPI and a mouse anti-GFP antibody (Sigma-Aldrich). The primary antibody was detected with the Alexa Fluor 594 Signal Amplification Kit for Mouse Antibodies (Molecular Probes), as per the manufacturer's instructions. The production of GFP by iGFP *Lm* in BHI broth was determined by adding 10 mM IPTG to overnight cultures of bacteria, incubating at 37°C and fixing bacteria at 10–30 min intervals. Bacteria were stained with mouse anti-GFP and then Alexa Fluor 594 antibodies and DAPI. Bacteria were centrifuged onto 13 mm coverslips at 700 r.p.m. for 5 min iGFP *Lm* and infected cells were mounted on glass slides with Prolong Antifade (Molecular Probes). For each coverslip, 100 DAPI-labelled bacteria were scored for Alexa Fluor 594 staining.

Acknowledgements

The authors thank Mary O'Riordan and Daniel Portnoy for their valuable suggestions. This work was partially supported by US Public Health Service Grants AI35950 (J.A.S.) and AI53669 (D.E.H.) from the National Institutes of Health.

References

Alvarez-Dominguez, C., and Stahl, P.D. (1999) Increased expression of Rab5a correlates directly with accelerated

maturation of *Listeria monocytogenes* phagosomes. *J Biol Chem* **274**: 11459–11462.

Alvarez-Dominguez, C., Roberts, R., and Stahl, P.D. (1997) Internalized *Listeria monocytogenes* modulates intracellular trafficking and delays maturation of the phagosome. *J Cell Sci* **110**: 731–743.

Beauregard, K.E., Lee, K.D., Collier, R.J., and Swanson, J.A. (1997) pH-dependent perforation of macrophage phagosomes by listeriolysin O from *Listeria monocytogenes*. *J Exp Med* **186**: 1159–1163.

de Chastellier, C., and Berche, P. (1994) Fate of *Listeria monocytogenes* in murine macrophages: evidence for simultaneous killing and survival of intracellular bacteria. *Infect Immun* **62**: 543–553.

Conte, M.P., Petrone, G., Longhi, C., Valenti, P., Morelli, R., Superti, F., and Seganti, L. (1996) The effects of inhibitors of vacuolar acidification on the release of *Listeria monocytogenes* from phagosomes of Caco-2 cells. *J Med Microbiol* **44**: 418–424.

Cossart, P., and Lecuit, M. (1998) Interactions of *Listeria monocytogenes* with mammalian cells during entry and actin-based movement: bacterial factors, cellular ligands and signaling. *EMBO J* **17**: 3797–3806.

Dancz, C.E., Haraga, A., Portnoy, D.A., and Higgins, D.E. (2002) Inducible control of virulence gene expression in *Listeria monocytogenes*: temporal requirement of listeriolysin O during intracellular infection. *J Bacteriol* **184**: 5935–5945.

Deretic, V., and Fratti, R.A. (1999) *Mycobacterium tuberculosis* phagosome. *Mol Microbiol* **31**: 1603–1609.

Desjardins, M., Huber, L.A., Parton, R.G., and Griffiths, G. (1994) Biogenesis of phagolysosomes proceeds through a sequential series of interactions with the endocytic apparatus. *J Cell Biol* **124**: 677–688.

Gillooly, D.J., Morrow, I.C., Lindsay, M., Gould, R., Bryant, N.J., Gaullier, J.M., et al. (2000) Localization of phosphatidylinositol 3-phosphate in yeast and mammalian cells. *EMBO J* **19**: 4577–4588.

Glomski, I.J., Gedde, M.M., Tsang, A.W., Swanson, J.A., and Portnoy, D.A. (2002) The *Listeria monocytogenes* hemolysin has an acidic pH optimum to compartmentalize activity and prevent damage to infected host cells. *J Cell Biol* **156**: 1029–1038.

Glomski, I.J., Decatur, A.L., and Portnoy, D.A. (2003) *Listeria monocytogenes* mutants that fail to compartmentalize listeriolysin O activity are cytotoxic, avirulent, and unable to evade host extracellular defenses. *Infect Immun* **71**: 6754–6765.

Gordon, A.H., Hart, P.D., and Young, M.R. (1980) Ammonia inhibits phagosome-lysosome fusion in macrophages. *Nature* **286**: 79–80.

Hakansson, A., Bentley, C.C., Shakhnovic, E.A., and Wesels, M.R. (2005) Cytolysin-dependent evasion of lysosomal killing. *Proc Natl Acad Sci USA* **102**: 5192–5197.

Hashim, S., Mukherjee, K., Raju, M., Basu, S.K., and Mukhopadhyay, A. (2000) Live *Salmonella* modulate expression of Rab proteins to persist in a specialized compartment and escape transport to lysosomes. *J Biol Chem* **275**: 16281–16288.

Henry, R.M., Hoppe, A.D., Joshi, N., and Swanson, J.A. (2004) The uniformity of phagosome maturation in macrophages. *J Cell Biol* **164**: 185–194.

Higgins, D.E., Buchrieser, C., and Freitag, N.E. (2005) Genetic tools for use with *Listeria monocytogenes*. In *Gram-Posi-*

- tive Pathogens*, 2nd edition. Fischetti, V.A., Novick, R.P., Ferretti, J.J., Portnoy, D.A., and Rood, J.I. (eds). New York: American Society for Microbiology Press (in press).
- Hoppe, A.D., and Swanson, J.A. (2004) Cdc42, Rac1, and Rac2 display distinct patterns of activation during phagocytosis. *Mol Biol Cell* **15**: 3509–3519.
- Jones, S., and Portnoy, D.A. (1994) Intracellular growth of bacteria. *Methods Enzymol* **236**: 463–467.
- Lauer, P., Chow, M.Y., Loessner, M.J., Portnoy, D.A., and Calendar, R. (2002) Construction, characterization, and use of two *Listeria monocytogenes* site-specific phage integration vectors. *J Bacteriol* **184**: 4177–4186.
- Loessner, M.J., Kramer, K., Ebel, F., and Scherer, S. (2002) C-terminal domains of *Listeria monocytogenes* bacteriophage murein hydrolases determine specific recognition and high-affinity binding to bacterial cell wall carbohydrates. *Mol Microbiol* **44**: 335–349.
- Mellman, I., Fuchs, R., and Helenius, A. (1986) Acidification of the endocytic and exocytic pathways. *Annu Rev Biochem* **55**: 663–700.
- Myers, J.T., Tsang, A.W., and Swanson, J.A. (2003) Localized reactive oxygen and nitrogen intermediates inhibit escape of *Listeria monocytogenes* from vacuoles in activated macrophages. *J Immunol* **171**: 5447–5453.
- Peters, C., and von Figura, K. (1994) Biogenesis of lysosomal membranes. *FEBS Lett* **346**: 146–150.
- Peters, C., and Mayer, A. (1998) Ca²⁺/calmodulin signals the completion of docking and triggers a late step of vacuole fusion. *Nature* **396**: 575–580.
- Portnoy, D.A., Jacks, P.S., and Hinrichs, D.J. (1988) Role of hemolysin for the intracellular growth of *Listeria monocytogenes*. *J Exp Med* **167**: 1459–1471.
- Portnoy, D.A., Tweten, R.K., Kehoe, M., and Bielecki, J. (1992) Capacity of listeriolysin O, streptolysin O, and perfringolysin O to mediate growth of *Bacillus subtilis* within mammalian cells. *Infect Immun* **60**: 2710–2717.
- Portnoy, D.A., Auerbuch, V., and Glomski, I.J. (2002) The cell biology of *Listeria monocytogenes* infection: the intersection of bacterial pathogenesis and cell-mediated immunity. *J Cell Biol* **158**: 409–414.
- Prada-Delgado, A., Carrasco-Marin, E., Bokoch, G.M., and Alvarez-Dominguez, C. (2001) Interferon-gamma listericidal action is mediated by novel Rab5a functions at the phagosomal environment. *J Biol Chem* **276**: 19059–19065.
- Prada-Delgado, A., Carrasco-Marin, E., Pena-Macarro, C., Del Cerro-Vadillo, E., Fresno-Escudero, M., Leyva-Cobian, F., and Alvarez-Dominguez, C. (2005) Inhibition of Rab5a exchange activity is a key step for *Listeria monocytogenes* survival. *Traffic* **6**: 252–265.
- Pryor, P.R., Mullock, B.M., Bright, N.A., Gray, S.R., and Luzio, J.P. (2000) The role of intraorganellar Ca(2+) in late endosome-lysosome heterotypic fusion and in the reformation of lysosomes from hybrid organelles. *J Cell Biol* **149**: 1053–1062.
- Roberts, R.L., Barbieri, M.A., Ullrich, J., and Stahl, P.D. (2000) Dynamics of rab5 activation in endocytosis and phagocytosis. *J Leukoc Biol* **68**: 627–632.
- Shen, A., and Higgins, D.E. (2005) The 5' untranslated region-mediated enhancement of intracellular listeriolysin O production is required for *Listeria monocytogenes* pathogenicity. *Mol Microbiol* **57**: 1460–1473.
- Shiloh, M.U., MacMicking, J.D., Nicholson, S., Brause, J.E., Potter, S., Marino, M., et al. (1999) Phenotype of mice and macrophages deficient in both phagocyte oxidase and inducible nitric oxide synthase. *Immunity* **10**: 29–38.
- Stenmark, H., Aasland, R., and Driscoll, P.C. (2002) The phosphatidylinositol 3-phosphate-binding FYVE finger. *FEBS Lett* **513**: 77–84.
- Tweten, R.K., Parker, M.W., and Johnson, A.E. (2001) The cholesterol-dependent cytolysins. *Curr Top Microbiol Immunol* **257**: 15–33.
- van Weert, A.W., Dunn, K.W., Gueze, H.J., Maxfield, F.R., and Stoorvogel, W. (1995) Transport from late endosomes to lysosomes, but not sorting of integral membrane proteins in endosomes, depends on the vacuolar proton pump. *J Cell Biol* **130**: 821–834.
- Zimmer, M. (2002) Green fluorescent protein (GFP): applications, structure, and related photophysical behavior. *Chem Rev* **102**: 759–781.